Theory of the spin Hall effect in metal oxide structures

I. Hajzadeh, B. Rahmati, G. R. Jafari, and S. M. Mohseni[*]

Faculty of Physics, Shahid Beheshti University, Tehran 19839, Iran

The spin Hall effect is considered a phenomenon in which a charge current is converted to a spin current due to the spin-orbit coupling (SOC). Recently, large values of the spin Hall angle (SHA), as the conversion efficiency between spin and charge currents, were observed in metal oxide structures in ferromagnetic/metal (FM/M) oxide bilayers, although their underlying mechanisms are ambiguous. The present study aims to analytically indicate that a mixed region of metal and oxide formed at the metal/oxide interface includes the surface oxide charge, which allows for introducing an SOC term in the electron Hamiltonian. Based on the results, the SHA increases by two orders of magnitude in a Cu/oxide thin film through the side jump and skew scattering mechanisms, reaching that of heavy metals. In addition, a comprehensive model is provided for the influence of oxidation on the SHA and spin-orbit torques (SOTs) in FM/M structures. We find that the magnitude of SOTs is greatly dependent on (i) the surface oxidation condition, (ii) the current flow path, and (iii) the electronic interface condition. The model represented in the present study is regarded as a promising model and prediction mechanism which explains recent observations. The findings can be implemented in generating spin current without any use of external magnetic fields and heavy metals in spintronic devices.

I. INTRODUCTION

The spin Hall effect (SHE) has been highly considered one of the most attractive topics in spintronics because of the generation and detection of spin current in nonmagnetic metals and also the possibility to implement in the future miniaturized spintronic architectures for which no magnetic field is required. This effect was first predicted by Dyakonov and Perel in 1971 [1], revived by Hirsch in 1999 [2], observed optically in semiconductors and two-dimensional electron gases [3,4], and probed electrically in metallic conductors [5]. In order to benefit from this effect, materials with a large spin Hall angle (SHA), as the conversion efficiency between spin and charge currents, are required to have the capability of converting a longitudinal charge current to a transverse spin current. Materials with intrinsically strong spin-orbit coupling (SOC) represent large SHAs and are called heavy metals (HMs), such as Pt, Ir, and Bi. However, it can impose a limitation on selecting the materials for application in spintronic devices such as spin-Hall oscillators [6], SHE transistors [7], and spin photo-detectors [8]. On the other hand, light metals are inappropriate for such spintronic devices due to their weak SOC. Hence, a question raised here is how the SHE is enhanced in metals, which has attracted a lot of attention in spintronics.

Attempts have been made to circumvent this drawback in light metals. For example, doping metals with a HM impurity was found to be one of the solutions to achieve a large SHA [9–14], and light metals surface roughness was reported to control the SHA [15,16]. Another suggestion was to use the

interfacial Rashba spin-orbit coupling (IRSOC) as an alternative mechanism to generate a large SHA [17–19]. Recently, a large number of experimental reports indicated that the SHA can be enhanced through metal surface oxidation [20–29]. However, based on these experimental reports, the reason for increasing the SHA through surface oxidation is not well understood, and further investigations are needed. Theoretically, a giant spin Hall conductivity emerges in the presence of IRSOC when a normal metallic thin film is sandwiched by oxide layers [17]. The result is inconsistent with the experimental reports indicating that the SHE induced by surface oxidation does not occur due to IRSOC [22,23,25,28]. As already mentioned, uncovering the physical mechanisms which can potentially predict the methods for increasing the SHA in the metal is highly desirable. Furthermore, the SHE generated experimentally in the interface between oxide and different materials lacks a theoretical framework or clear underlying mechanism.

In this paper, a different source of SHE is proposed based on scattering the electrons from the surface oxide charges which are present as inhomogeneous (INHO) surface oxidation within the metal thin films and predict a significant increase in the SHA. In addition, a mixed region of a metal and oxide layer, which is formed at the metal/oxide interface and is contained by surface oxide charges, is presented as the main reason for increasing the SHA in metals exposed to oxygen. Obviously, such surface charges can be present adjacent to any metal/dielectric interfaces, such as nitrate and sulfide, and the metal oxidation used in the present study can easily be accessed in experiments. In fact, the present study focuses on the naturally or inhomogeneously oxidized Cu thin film when side jump and skew scattering contributions are available. The results indicate that SHA can be enhanced by two orders of magnitude through the INHO surface oxidation compared to

―――――
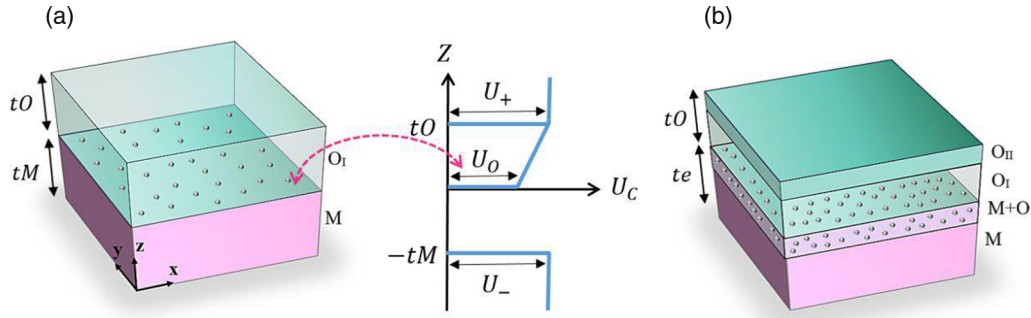[*]Corresponding author: m-mohseni@sbu.ac.ir; majidmohseni@gmail.com

FIG. 1. (a) A schematic illustration of a HO metal oxide layer (M/O$_I$; left) and the confining potential U_C [Eq. (1)] along the confinement direction (i.e., z axis; right). The location of surface oxide charges is shown by dashed red arrows. (b) A schematic illustration of an INHO metal oxide layer (M/O$_I$/O$_{II}$) which includes the mixed region (M + O) containing the surface oxide charges.

that of HM bulk. Further, the dependence of film thickness on the SHA induced by the surface oxide charges is evaluated. The results indicate that its behavior is opposite to the bulk spin-orbit materials. This unique characteristic will make it possible to distinguish the surface oxidation origin of the SHE in future experiments. The main application of the SHE is a torque exertion on neighboring magnetic moments for, e.g., spin-orbit torque (SOT) for magnetization reversal. Here, a comprehensive model is provided for the effect of oxidation on the SHE and SOT in ferromagnetic/metal (FM/M) oxide structures.

The rest of this paper is organized as follows. Homogeneous (HO) and INHO metal surface oxidations are described in Sec. II. We present a theoretical description for a metal oxide thin film in Sec. III and obtain the spin Hall conductivity in Sec. IV. Finally, the results, discussions, and conclusions are presented in Sec. V.

II. HOMOGENEOUS AND INHOMOGENEOUS OXIDATIONS

A homogeneous metal oxide layer (M/O$_I$) is produced when the metal is completely oxidized in the presence of oxygen. The mechanisms of oxide growth are based on how the electrons and ions accelerate and move outward toward the oxide/oxygen interface [22,30–32]. By moving electrons and ions from the metal/oxide to oxide/oxygen interface, the surface (interface) oxide charges with charge density ρ are produced adjacent to the M/O$_I$ interface [Fig. 1(a)]. Such surface oxide charges are popular and have been generated in the semiconductors/oxide interface [32–36].

An inhomogeneous metal oxide layer is produced when the M/O$_I$ is exposed to excess oxygen like in a longer oxidation or natural oxidation process [22,30], which finally forms a different metal oxide phase adjacent to the oxide/oxygen interface (M/O$_I$/O$_{II}$). Thus, as illustrated in Fig. 1(b), the potential barrier between the metal and the initial oxide phase is reduced, leading to the creation of a mixed region of metal and metal oxide. Based on the oxidation conditions, the mixed region including surface oxide charges can be established between the metal and initial oxide or between the metal and new metal oxide phase [30]. As an example, when a Cu thin film is exposed to oxygen, a Cu native oxide layer (HO metal oxide layer) is formed immediately after exposure as

described by the following reaction: $4Cu^+ + O_2 \rightarrow 2Cu_2O$. Under excess oxygen loading of Cu/Cu$_2$O, Cu electrons and ions move from the metal/oxide to oxide/oxygen interface and interact with oxygen atoms, leading to the creation of a CuO layer which can be described by the following reaction: $2Cu_2O + O_2 \rightarrow 4CuO$. Accordingly, a mixed region of metal and oxide is formed adjacent to the metal/oxide interface since the potential barrier is reduced and Cu electrons and ions moved from the metal/oxide interface. Hence, the excess oxidation process (or natural oxidation process) creates an INHO or duplex-type oxidized structure and forms a mixed region in Cu thin film as Cu/Cu$_2$O/CuO [22,30].

III. MODEL

We first consider a HO metal oxide M/O$_I$ layer structure [Fig. 1(a)]. A film with dimensions $A \times (t_M + t_O)$ is confined in the z direction and extended in the $r = (x, y)$ direction, where A represents the area of the film and t_M (t_O) indicates the thickness of the M (O) film. The surface oxide charges are located adjacent to the M/O$_I$ interface. In fact, the M/O$_I$ interface is in the r plane at $z = 0$. The Hamiltonian for this system is given by

$$H = \frac{p^2}{2m} + U_C + u + u_{so}. \tag{1}$$

The first term is the kinetic energy with electron mass m and momentum operator p. $U_C = U_-\Theta(-z - t_M) + U_O + U_+\Theta(z - t_O)$ indicates the confining potential of the metal film between vacuum and O [34], with $U_O \sim U_0[\Theta(z) - \Theta(z - t_O)]$, where $U_0(U_+, U_-)$ represents the height of the potential barrier at $z = 0$ ($z = t_O$, $-t_M$) and $\Theta(z)$ is considered the Heaviside step function. In addition, $u = -e\phi$ is the surface oxide charge potential, where ϕ represents the electrostatic potential and e is regarded as the electron charge, i.e., $\nabla^2\phi = \rho/\epsilon$, with $\epsilon = \kappa\epsilon_0$, where ϵ_0 and κ are the vacuum permittivity and dielectric constant, respectively [33–36] (refer to Refs. [34,35] for more information about ϕ). The last term in Eq. (1) is the spin-orbit interaction potential due to the surface oxide charges, $u_{so} = \eta\,\hat{\sigma} \cdot [\nabla u \times (ip/\hbar)]$, where η is the SOC parameter, $\hat{\sigma} = (\sigma_x, \sigma_y, \sigma_z)$ indicates the Pauli spin operator, and $\hbar$ is the reduced Planck constant, i.e., when an electron with velocity p/m passes through the metal/oxide interface in the presence of an electric field

generated by surface charges (∇u), which feels an effective magnetic field leading to the SOC.

In the present study, u and u_{so} are considered perturbations to $H_0 = (p^2/2m) + U_C$, and for simplicity, $U_0 \gg E_F$, where E_F represents the Fermi energy and takes the limit $U_\pm \to \infty$. Now, we consider the INHO case is generated; therefore, the potential barrier is reduced [Fig. 1(b)]. Thus, the electrons can penetrate the mixed region with a depth $t = \sqrt{\hbar^2/2U_0}$, and accordingly, the effective thickness becomes $t_e = t_M + t$. Further, the eigenenergies and eigenstates related to H_0 are obtained for spins with $s = \pm(\uparrow\downarrow)$, in-plane wave vector k, and a transverse channel index n,

$$E_{kns} = \frac{\hbar^2 k^2}{2m} + E_n + \frac{t \, u_{ox}}{t_M U_0}\left(1 + \eta s \frac{k}{t_e}\right)E_n,$$

$$|kns\rangle = \sqrt{\frac{2}{\Omega}} \, \sin[k_n(z + t)] \exp(ik \cdot r)|s\rangle, \quad (2)$$

where u_{ox} indicates the magnitude of scattering the electrons from surface oxide charges, $E_n = \hbar^2 k_n^2/2m$, $\Omega = At_e$ represents the film volume, $k_n = n\pi/t_e$, and $|s\rangle$ are considered the eigenspin states with $\hat{\sigma}|s\rangle = s|s\rangle$.

The two last terms in Eq. (1) can lead to a transition between the unperturbed eigenstates. The transition probability is provided by Fermi's golden rule,

$$P(|kns\rangle \to |k'n's'\rangle) = \frac{2\pi}{\hbar} \langle|T_{k'n's',kns}|^2\rangle_{ave}$$
$$\times \delta(E_{k'n's'} - E_{kns}), \quad (3)$$

where $T_{k'n's',kns} = \langle k'n's'|T|kns\rangle$ indicates the scattering matrix element and invokes the scattering potentials u, u_{so} and $\langle\cdots\rangle_{ave}$ denotes the average over the surface oxide charge positions. Based on the Born approximation, the T matrix element is found up to second order as follows:

$$T_{k'n's',kns} = \left[u_{k'n'}^{kn} + \sum_{k''n''s''} \frac{u_{k'n'}^{k''n''} u_{k''n''}^{kn}}{E_{kns} - E_{k''n''s''} + i\lambda}\right]$$
$$\times \delta_{s's} + i\eta\sigma_{s's}u_{k'n'}^{kn}(\hat{k}' \times \hat{k}), \quad (4)$$

where

$$u_{k'n'}^{kn} = \langle k'n'|u|kn\rangle = \left(\frac{\pi e^2 t}{q\epsilon}\right)\sum_{j=1}^{N_{ox}}\left(\frac{2}{\Omega}\right)\exp(iq \cdot r_j)$$
$$\times \sin[k_{n'}(z_j + t)]\sin[k_n(z_j + t)], \quad (5)$$

where λ represents an infinitesimal positive constant, δ indicates the Kronecker delta, $\sigma_{s's} = \langle s'|\hat{\sigma}|s\rangle$, $q = k - k'$, and N_{ox} is the number of surface oxide charges.

After averaging over surface oxide charge positions, the scattering probability indicated symmetric and asymmetric contributions. Then, the charge and spin relaxation time is found due to surface oxide charges by using the symmetric part of the probability,

$$\frac{1}{\tau_{kn}} = \sum_{k'n's'} P_{sym}(|kns\rangle \to |k'n's'\rangle)(1 - \hat{k}' \cdot \hat{k})$$
$$= \frac{1}{\tau_0(t)}\left(1 + \frac{2(\eta k_F^2)^2}{3}\right), \quad (6)$$

where

$$\frac{1}{\tau_0(t)} = \frac{2\pi^2}{\hbar}\frac{n_{ox}}{n_{eff}}\frac{3n_c}{4E_F}\frac{(n_c + \frac{1}{2})}{\chi}\left(\frac{e^2 t \, n_{eff}}{2k_F\epsilon}\right)^2, \quad (7)$$

where k_F represents the Fermi momentum, $n_{ox} = N_{ox}/\Omega$ indicates the concentration of surface oxide charges, $n_c = [\chi]$, $\chi = k_F t_e/\pi$, and $[\cdots]$ denotes the integer part of a number. Further, we define $n_{eff} = n_s t E_F/t_M U_0$, with $n_s = k_F^3/3\pi^2$, where n_{eff} represents the concentration of electrons which can be penetrated to the mixed region and scattered from surface oxide charges.

IV. SPIN HALL CONDUCTIVITY

The spin Hall conductivity σ_{SH} is proportional to the sum of the side jump α_{side} and skew scattering α_{skew} contributions according to $\sigma_{SH} = (\alpha_{side} + \alpha_{skew})\sigma_N$ [37], where σ_N is the in-plane conductivity. By using the Boltzmann equation, the in-plane longitudinal charge current in the presence of the electric field $E\hat{e}$, where $\hat{e}$ is a unit vector along the electric field, can be obtained with $J = \sigma_N E = (2e/\Omega)\sum_{kns}(\hbar k/m)g_{kns}$. Here, $g_{kns} = -e\tau_0(t)(\hbar k/m)\delta(E_{kns} - E_F)E\hat{e} \cdot \hat{k}$ describes the out-of-equilibrium distribution function. Then

$$\sigma_N = \frac{3\sigma_0}{2}\frac{n_c}{\chi}\frac{\tau_0(t)}{\tau_0}\left[1 - \frac{S(n_c)}{n_c\chi^2}\right], \quad (8)$$

where $\sigma_0 = n_s e^2 \tau_0/m$ represents the bulk conductivity in the Drude model and $S(n_c) = \sum_{n=1}^{n_c} n^2$ [38].

Regarding the asymmetric part of the scattering probability $P_{asym}(|kns\rangle \to |k'n's'\rangle)$ in Eq. (3), a term producing transverse scattering at the Fermi level is obtained as follows [39]:

$$\sum_{k'n's'} P_{asym}(|kns\rangle \to |k'n's'\rangle)g_{k'n's'}$$
$$= es\alpha_{skew}E\hat{e} \cdot (\hat{k} \times \hat{z}), \quad (9)$$

where $\hat{z}$ indicates the polarization vector. The cross terms between the symmetric and asymmetric parts of the T matrix contribute only to Eq. (9), and accordingly, α_{skew} becomes

$$\alpha_{skew} = \frac{\eta k_F^2}{E_F}u_{ox}n_c, \quad (10)$$

where $u_{ox} = \pi e^2 t \, n_{eff}/k_F\epsilon$.

Regarding the side jump contribution, we need to consider only the following expression for the anomalous velocity $\alpha_a(k, n, s)$ [39,40]:

$$\alpha_a(k, n, s) = -\pi \sum_{k'n's'} \delta(E_{k'n's'} - E_{kns})$$
$$\times \text{Im}(T_{k'n's',kns})^\dagger \nabla_{k'} T_{k'n's',kns}. \quad (11)$$

By using Eqs. (4) and (11), $\alpha_a(k, n, s) = \alpha_{side}s\hat{k} \times \hat{z}$ is obtained, where

$$\alpha_{side} = \frac{\hbar\eta k_F^2}{2E_F\tau_0(t)}. \quad (12)$$

By using Eqs. (8), (10), and (12) and averaging over the surface oxide charge distribution, the spin Hall conductivity attributed to skew scattering ($\sigma_{SH}^{skew} = \alpha_{skew}\sigma_N$) and the side
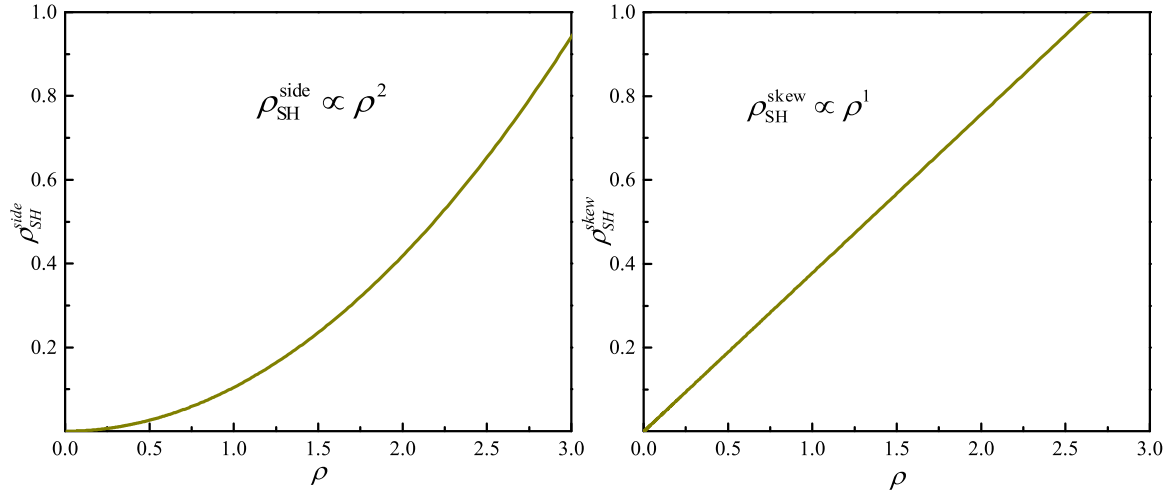
FIG. 2. Spin Hall resistivity $\rho_{SH} = \sigma_{SH}/\sigma_N^2$ as a function of resistivity $\rho = 1/\sigma_N$ for the side jump (left) and skew scattering (right) for $t_M = 10$ nm, $t = 2$ nm, $\bar{\eta} = \eta k_F^2 = 0.5$, $k_F = 1.36 \times 10^{10}$/m, $E_F = 7$ eV, $\kappa = 5$, and $n_s = 10^{21}$ cm^{-3}.

jump ($\sigma_{SH}^{side} = \alpha_{side}\sigma_N$) is found as follows:

$$\sigma_{SH}^{skew} = \frac{\eta k_F^2}{E_F} u_{ox} n_c \sigma_N, \tag{13}$$

$$\sigma_{SH}^{side} = \frac{e^2\eta}{\hbar} \frac{3n_s}{2} \frac{n_c}{\chi} \left[1 - \frac{S(n_c)}{n_c \chi^2} \right]. \tag{14}$$

The contribution of the side jump term in the conductivity is independent of the surface oxide charges. On the contrary, the conductivity due to the skew scattering relies on the strength, sign, and distribution of the surface oxide charge. The skew scattering contribution is dominant in the SHE when the concentration of the surface oxide charges has a narrow distribution with definite sign, while the potentials are distributed with similar portions of positive and negative contributions for the surface oxide charge and their average value vanishes ($u_{ox} \approx 0$), leading to the dominance of the side jump contribution.

V. RESULTS AND DISCUSSION

The skew scattering (side jump) spin Hall resistivity ρ_{SH}^{skew} (ρ_{SH}^{side}), originating from the metal oxide structure, is given by the skew scattering (side jump) conductivity equations (13) and (14) divided by σ_N^2. Figure 2 illustrates the plot of ρ_{SH}^{skew} (ρ_{SH}^{side}) as a function of ρ with the slope of a power-law fit, which is 1 (2), i.e., ρ_{SH}^{skew} (ρ_{SH}^{side}) $\sim \rho^1$ (ρ^2). In conventional bulk SHE, the relation between the spin Hall resistivity and the longitudinal resistivity is $\rho_{SH} = a\rho + b\rho^2$ [37], where the linear and quadratic terms are due to skew scattering and side jump mechanisms, respectively. On the other hand, the SHE in the present model arises from a significant enhancement of the SOC in the Cu layer through the INHO oxidation. Therefore, it is concluded that the SHE induced by INHO oxidizing the metal has the same behavior as the SHE related to the bulk of the metal.

The SHA is proportional to σ_{SH} divided by σ_N. It is assumed that the surface oxide charges are randomly distributed in the mixed region. Hence, the skew scattering term becomes zero, $\alpha_{skew} = 0$ [16,37]. The effect of the thickness t in the

mixed region of metal and metal/oxide on the SHA for Cu film is plotted in the left panel of Fig. 3 for three different values of the dielectric constant. Different dielectric constants can be achieved through oxygen concentration or by using other dielectric materials such as nitrates, sulfides, etc. The SHA increases with increasing t because the electrons can penetrate farther and be scattered more from surface oxide charges in the mixed region by increasing the thickness of this region. In other words, the density of the effective carrier increases by increasing the thickness of the mixed region, i.e., $n_{eff} = n_s t E_F / t_M U_0$. Furthermore, by increasing t, a decrease occurs in the potential U_0 in the M/O$_I$ interface, or $t \sim U_0^{-1/2}$, leading to the penetration of more electrons into the mixed region. The left panel of Fig. 3 displays the SHA dependence on the electron concentration. In addition, the electrical resistivity decreases by increasing the metal layer thickness t_M [41]. Thus, electrons prefer to pass through the metal layer instead of penetrating to the mixed region. In other words, a decrease occurs in the SHA, which can potentially be examined through experiments to distinguish the source of the SHE.

The right panel of Fig. 3 illustrates the dependence of the dielectric constant κ of the mixed region on the SHA for three different thicknesses of the mixed region. For all cases, the SHA decreases with increasing κ because the surface oxide charges and the generated electric field due to the surface oxide charges decrease by increasing the dielectric constant. Thus, the last term in Eq. (1), u_{so}, leads to a decrease in the SHA. The right panel of Fig. 3 shows the SHA dependence on the concentration of surface oxide charges. As illustrated, the SHA is enhanced by over two orders of magnitude for the Cu layer, which reaches the SHA in the bulk of HMs such as Pt [SHA $\sim O(0.1)$]. This occurs by increasing the thickness of the mixed region obtained by tuning the surface oxidation concentration. Based on the experimental reports for natural oxidation, the SHA increases by increasing the INHO surface oxidation in metal thin films, which seems to be consistent with the aforementioned arguments [20,22,23,25,28].

Now, we use the determined value of SHA in the SOT applied to a FM layer in FM/M bilayer structures, where the
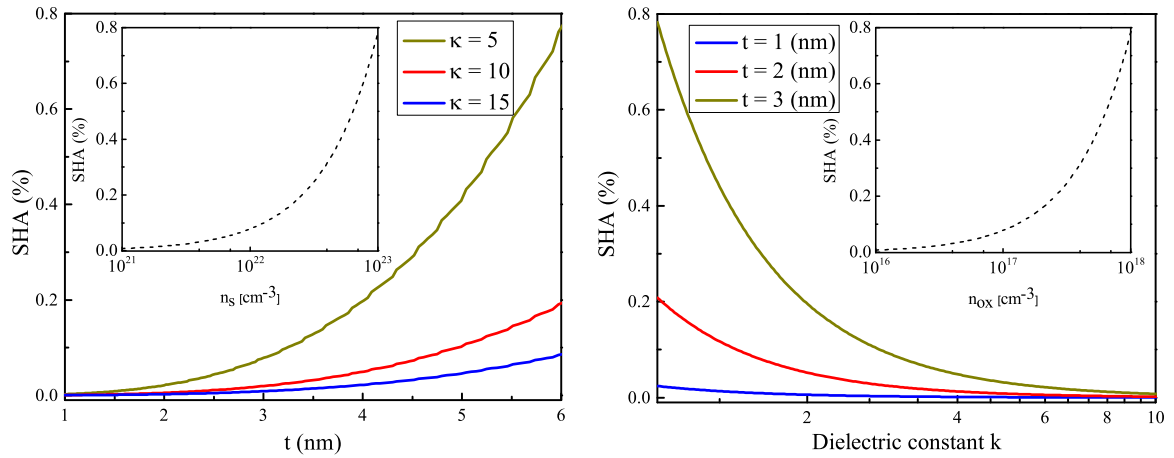
FIG. 3. Left: The SHA (%) for a Cu film, $t_M = 10$ nm, $\bar{\eta} = 0.5$, $k_F = 1.36 \times 10^{10}$/m, and $E_F = 7$ eV as a function of t for three cases of dielectric constants, $n_s = 10^{23}$ cm^{-3}, and $n_{ox} = 10^{17}$ cm^{-3}. The inset shows the SHA (%) dependence on the electron concentration n_s with $t = 3$ nm and $n_{ox} = 10^{18}$ cm^{-3}. Right: The SHA (%) for a Cu film, $t_M = 10$ nm, $\bar{\eta} = 0.5$, $k_F = 1.36 \times 10^{10}$/m, and $E_F = 7$ eV as a function of dielectric constant for three cases of t, $n_s = 10^{22}$ cm^{-3}, and $n_{ox} = 4 \times 10^{16}$ cm^{-3}. The inset demonstrates the SHA (%) dependence on the surface oxide charge concentration n_{ox} with $t = 3$ nm and $n_s = 10^{23}$ cm^{-3}.

M or FM layer is oxidized [20–23,25,28,29]. In such bilayers, two mechanisms have been suggested as candidate sources of SOTs, and they are (i) the Rashba-Eldestein effect (REE) arising from electronic discontinuities at the interface(s) of two distinct materials and (ii) the SHE results from the effect of an incident transverse spin current on the FM. Both mechanisms can exert damplike (DL) SOT τ_{DL} and fieldlike (FL) SOT τ_{FL} on the FM layer, characterized by DL SOT and FL SOT efficiencies ξ_{DL} and ξ_{FL}, respectively. The SHE is generally expected to exert a larger DL SOT than the FL one, in contrast to the REE. Identifying the source of SOT is an obstacle in such commonly used bilayers. Hence, a comprehensive understanding of the influence of oxidation on the SHA and $\xi_{DL(FL)}$ should be provided in a way that it can be used to distinguish the SOT source.

We discuss four different structures that can be considered for surface oxidation in FM/M bilayers (Fig. 4). In the first two structures, the top layer [Figs. 4(a) and 4(b)] is oxidized,
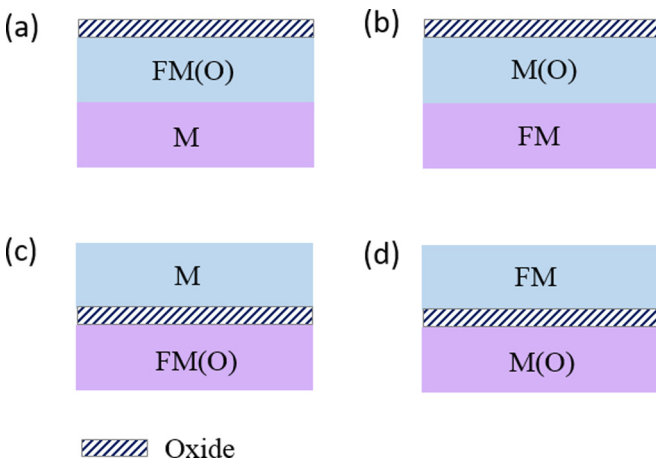
and in the second two, the bottom layer (and the interface) is oxidized [Figs. 4(c) and 4(d)]. The magnitude and even the sign of τ_{DL} and τ_{FL} are greatly dependent on (i) the surface oxidation condition, (ii) the current flow path, and (iii) the electronic interface condition. For natural surface oxidation (INHO), the resistivity of the oxidized layer in comparison to its adjacent layer (in a bilayer) is in a way that the current can pass through the mixed region [22] containing surface oxide charges [Figs. 4(a) and 4(b)]. Hence, the SHE induced by surface oxide charges is the source of SHA enhancement ($\tau_{DL} > \tau_{FL}$). If the oxidation of the surface is HO, the current passes around the oxide region, and the interface conditions of the two materials are such that they are electronically discontinuous [Figs. 4(c) and 4(d)], then REE is the source of the increase in SHA ($\tau_{DL} < \tau_{FL}$). In addition, if $\tau_{DL} \approx \tau_{FL}$, then it can be suggested that both mechanisms may play a significant role in SOT increasing (Figs. 4(c) and 4(d); in a way that the interfaces are naturally oxidized, i.e., the INHO case [23]).

Now, we consider the most important experimental reports up to now and try to resolve all the issues brought up in them. Qiu *et al.* observed that τ_{DL} increases as a result of surface oxidation in Pt/CoFeB(O) (where CoFeB is the top layer [Fig. 4(a)] and is naturally oxidized) [20]. They found that the sign of τ_{DL} changes with increasing surface oxidation. They believed that by oxidation of CoFeB, a new SOT source would be created without being aware of its theoretical mechanism. Based on our findings, by passing a portion of current through the mixed region, the SHE induced by surface oxide charges occurs, and $\tau_{DL} > \tau_{FL}$. The SHA increases with surface oxidation (mixed region) thickness t, while a small change in the thickness of CoFeB has a negligible effect on the SHA and τ_{DL}, all consistent with the reported experiment [20]. Furthermore, with increasing thickness of the CoFeB layer, the resistance decreases; thus, a small amount of the current passes through the mixed region, and hence, τ_{DL} decreases. The sign change of DL SOT with increases in surface oxidation could be caused by the change in the electric field

FIG. 4. A schematic illustration of different FM/M oxide bilayer structures.

direction [42] induced by surface oxide charges. In this case, DL SOT induced by surface oxide charges can have a sign opposite to DL SOT due to the bulk Pt, and the competition between these two terms can change the sign of DL SOT.

Demasius *et al.* reported an increase in the SHA and τ_{DL} via surface oxidation [21]. In their W(O)/CoFeB, W is the bottom layer [Fig. 4(d)], the oxidation of the surface is HO, and no mixed region is present [Fig. 1(a)]. Based on the electronic discontinuities at the interface [Fig. 4(d)], the REE at the interface of W(O)/CoFeB is the main source of the enhancement of SHA and τ_{DL}. It was later pointed out that due to the Berry phase effect, the τ_{DL} due to REE can be comparable to the τ_{DL} induced by SHE [43,44]. Moreover, significant changes and even a sign change in the FL SOT in oxidation interfaces were reported due to REE [24,26,29,45], which can be attributed to the variation of the spin-dependent disorder scattering [29].

An *et al.* investigated the effect of oxidation (both HO and INHO) of Cu, once as the bottom layer [Fig. 4(d)] and once as the top layer [Fig. 4(b)] in a Cu/NiFe bilayer [22]. In the first case, surface oxidation is HO, and Cu(O)/NiFe has electronic discontinuities [Fig. 4(d)]. Hence, it is expected that the REE is the source of the observed FL SOT. In the second case, in the NiFe/Cu(O) structure shown in Fig. 4(b), the Cu surface is oxidized once as INHO and once as HO. An increase of the DL SOT was observed for INHO, whereas no increase was seen in the HO case. Based on our findings, it can be concluded that the SHE induced by surface oxide charges is the source of the observed DL SOT. Our results are in good agreement with those in Ref. [22], where the SHA increases with surface oxidation (mixed region) thickness t and ξ_{DL} is negligible in a thicker Cu. As already mentioned, in the thicker Cu film, a small amount of the applied current flows in the mixed region, and most of the charge current flows in the nonoxidized Cu layer with the negligible SHE. Now, we proceed to a quantitative discussion of SHA and SOT for surface oxidation of Cu. The ξ_{DL} obtained from spin torque ferromagnetic resonance is related to SHA as $\xi_{DL} = T_{int}\theta_{SH}$ [46], where $0 < T_{int} < 1$ is the interfacial spin transparency and θ_{SH} is the SHA. We obtain, theoretically, $\theta_{SH} \sim 0.1$ with the same values used in Ref. [22] (Fig. 3) and suppose that $T_{int} = 0.7$; that is, 70% of the SHE-induced spin current is absorbed in the FM layer [46]. Thus, DL SOT efficiency becomes $\xi_{DL} \sim 0.07$, and this value is consistent with that seen in Ref. [22].

In conclusion, the SHE generated due to metal surface oxidation was predicted via establishing a mixed region of metal and oxide adjacent to the metal/oxide interface. This region including surface oxide charges can be experimentally made by manipulating the surface oxidation. By tuning the surface oxidation and manipulating the thickness in the mixed region and the dielectric constant, the SHA can be enhanced by over two orders of magnitude, reaching that of the bulk value in HM. Further, both the side jump and skew scattering mechanisms can contribute to SHE, depending on the distribution of the surface oxide charges. By comparing the SHAs determined due to the side jump and the skew scattering terms, we can approximately find optimal conditions to achieve a very large SHA. As an alternative approach, applying a gate voltage to control the SHA is suggested since the dielectric constant of the mixed region can affect the SHE significantly. Finally, the gate voltage can be used to expedite the migration of oxygen atoms [23,47] in such devices. Our achievements address how details of the surface oxidation can adjust the SHE in metals and also provide a comprehensive understanding of the influence of oxidation on the SHA and SOTs in FM/M oxide bilayers.

[1] M. Dyakonov and V. Perel, Phys. Lett. A **35**, 459 (1971).

[2] J. E. Hirsch, Phys. Rev. Lett. **83**, 1834 (1999).

[3] Y. Kato, R. Myers, A. Gossard, and D. Awschalom, Science **306**, 1910 (2004).

[4] J. Wunderlich, B. Kaestner, J. Sinova, and T. Jungwirth, Phys. Rev. Lett. **94**, 047204 (2005).

[5] S. O. Valenzuela and M. Tinkham, Nature (London) **442**, 176 (2006).

[6] T. Chen, R. K. Dumas, A. Eklund, P. K. Muduli, A. Houshang, A. A. Awad, P. Dürrenfeld, B. G. Malm, A. Rusu, and J. Åkerman, Proc. IEEE **104**, 1919 (2016).

[7] J. Wunderlich, B.-G. Park, A. C. Irvine, L. P. Zârbo, E. Rozkotová, P. Nemec, V. Novák, J. Sinova, and T. Jungwirth, Science **330**, 1801 (2010).

[8] J. Wunderlich, A. Irvine, J. Sinova, B. Park, L. Zârbo, X. Xu, B. Kaestner, V. Novák, and T. Jungwirth, Nat. Phys. **5**, 675 (2009).

[9] M. Gradhand, D. V. Fedorov, P. Zahn, and I. Mertig, Phys. Rev. Lett. **104**, 186403 (2010).

[10] Y. Niimi, M. Morota, D. H. Wei, C. Deranlot, M. Basletic, A. Hamzic, A. Fert, and Y. Otani, Phys. Rev. Lett. **106**, 126601 (2011).

[11] Y. Niimi, Y. Kawanishi, D. H. Wei, C. Deranlot, H. X. Yang, M. Chshiev, T. Valet, A. Fert, and Y. Otani, Phys. Rev. Lett. **109**, 156602 (2012).

[12] T.-Y. Chen, C.-T. Wu, H.-W. Yen, and C.-F. Pai, Phys. Rev. B **96**, 104434 (2017).

[13] R. Ramaswamy, Y. Wang, M. Elyasi, M. Motapothula, T. Venkatesan, X. Qiu, and H. Yang, Phys. Rev. Appl. **8**, 024034 (2017).

[14] D. V. Fedorov, C. Herschbach, A. Johansson, S. Ostanin, I. Mertig, M. Gradhand, K. Chadova, D. Ködderitzsch, and H. Ebert, Phys. Rev. B **88**, 085116 (2013).

[15] L. Zhou, V. L. Grigoryan, S. Maekawa, X. Wang, and J. Xiao, Phys. Rev. B **91**, 045407 (2015).

[16] I. Hajzadeh, S. M. Mohseni, S. M. S. Movahed, and G. R. Jafari, J. Phys.: Condens. Matter **30**, 195804 (2018).

[17] X. Wang, J. Xiao, A. Manchon, and S. Maekawa, Phys. Rev. B **87**, 081407(R) (2013).

[18] L. Sheng, D. N. Sheng, and C. S. Ting, Phys. Rev. Lett. **94**, 016602 (2005).

[19] H. Suzuura and T. Ando, Phys. Rev. B **94**, 035302 (2016).

[20] X. Qiu, K. Narayanapillai, Y. Wu, P. Deorani, D.-H. Yang, W.-S. Noh, J.-H. Park, K.-J. Lee, H.-W. Lee, and H. Yang, Nat. Nanotechnol. **10**, 333 (2015).

[21] K.-U. Demasius, T. Phung, W. Zhang, B. P. Hughes, S.-H. Yang, A. Kellock, W. Han, A. Pushp, and S. S. Parkin, Nat. Commun. **7**, 10644 (2016).

[22] H. An, Y. Kageyama, Y. Kanno, N. Enishi, and K. Ando, Nat. Commun. **7**, 13069 (2016).

[23] H. An, T. Ohno, Y. Kanno, Y. Kageyama, Y. Monnai, H. Maki, J. Shi, and K. Ando, Sci. Adv. **4**, eaar2250 (2018).

[24] M. Akyol, J. G. Alzate, G. Yu, P. Upadhyaya, K. L. Wong, A. Ekicibil, P. Khalili Amiri, and K. L. Wang, Appl. Phys. Lett. **106**, 032406 (2015).

[25] Y. Hibino, T. Hirai, K. Hasegawa, T. Koyama, and D. Chiba, Appl. Phys. Lett. **111**, 132404 (2017).

[26] S. Emori, U. Bauer, S. Woo, and G. S. Beach, Appl. Phys. Lett. **105**, 222401 (2014).

[27] Y. Ou, C.-F. Pai, S. Shi, D. C. Ralph, and R. A. Buhrman, Phys. Rev. B **94**, 140414(R) (2016).

[28] R. Enoki, H. Gamou, M. Kohda, and J. Nitta, Appl. Phys. Exp. **11**, 033001 (2018).

[29] T. Gao, A. Qaiumzadeh, H. An, A. Musha, Y. Kageyama, J. Shi, and K. Ando, Phys. Rev. Lett. **121**, 017202 (2018).

[30] I. Platzman, R. Brener, H. Haick, and R. Tannenbaum, J. Phys. Chem. C **112**, 1101 (2008).

[31] V. Drobny and L. Pulfrey, Thin Solid Films **61**, 89 (1979).

[32] N. Cabrera and N. Mott, Rep. Prog. Phys. **12**, 163 (1949).

[33] D. Chattopadhyay and H. Queisser, Rev. Mod. Phys. **53**, 745 (1981).

[34] T. Ning and C. Sah, Phys. Rev. B **6**, 4605 (1972).

[35] C. Sah, T. Ning, and L. Tschopp, Surf. Sci. **32**, 561 (1972).

[36] T. Ando, J. Phys. Soc. Jpn. **75**, 074716 (2006).

[37] S. Maekawa and T. Kimura, *Spin Current*, Semiconductor Science and Technology (Oxford University Press, Oxford, 2017), Vol. 22.

[38] N. Trivedi and N. W. Ashcroft, Phys. Rev. B **38**, 12298 (1988).

[39] A. Fert and P. M. Levy, Phys. Rev. Lett. **106**, 157208 (2011).

[40] P. Levy, Phys. Rev. B **38**, 6779 (1988).

[41] J. Kim, Y.-T. Chen, S. Karube, S. Takahashi, K. Kondou, G. Tatara, and Y. C. Otani, Phys. Rev. B **96**, 140409(R) (2017).

[42] G. Yu, P. Upadhyaya, Y. Fan, J. G. Alzate, W. Jiang, K. L. Wong, S. Takei, S. A. Bender, L.-T. Chang, Y. Jiang *et al.*, Nat. Nanotechnol. **9**, 548 (2014).

[43] E. van der Bijl and R. A. Duine, Phys. Rev. B **86**, 094406 (2012).

[44] H. Kurebayashi, J. Sinova, D. Fang, A. Irvine, T. Skinner, J. Wunderlich, V. Novák, R. Campion, B. Gallagher, E. Vehstedt *et al.*, Nat. Nanotechnol. **9**, 211 (2014).

[45] S. Emori, T. Nan, A. M. Belkessam, X. Wang, A. D. Matyushov, C. J. Babroski, Y. Gao, H. Lin, and N. X. Sun, Phys. Rev. B **93**, 180402 (2016).

[46] M.-H. Nguyen, D. C. Ralph, and R. A. Buhrman, Phys. Rev. Lett. **116**, 126601 (2016).

[47] U. Bauer, S. Emori, and G. S. Beach, Nat. Nanotechnol. **8**, 411 (2013).